New Jersey Institute of Technology

Digital Commons @ NJIT

Spring 5-31-2010

Comparison between different techniques of preprocessing for resting state fMRI analysis

Megha Girdhar
New Jersey Institute of Technology

Follow this and additional works at: https://digitalcommons.njit.edu/theses

Part of the Biomedical Engineering and Bioengineering Commons

ABSTRACT

COMPARISON BETWEEN DIFFERENT TECHNIQUES OF PREPROCESSING FOR RESTING STATE fMRI ANALYSIS

by
Megha Girdhar

Resting state functional connectivity as the name suggests is defined as significant temporal correlation between spatially distinct regions of the brain during rest. In this thesis, fMRI resting state dataset was analyzed using different available processing techniques with the same fMRI data to study differences between the various methods. All the imaging data from each of the subjects was processed in an identical fashion. The same method was used for detecting connectivity. The number of independent components in the data was used as the base to differentiate the effect of each of these methods. Independent component analysis was performed on each step after and before converting each dataset into MNI space to see the effect of normalization. In resting state fMRI study, different algorithms of motion correction showed no significant difference in the results. Temporal filtering by rectangular filter for particular bands of frequency showed no significant difference in the data analysis. Gaussian and Hamming windows however, work well for the required purpose. In case of spatial smoothing, Unsharp and Sobel filters which emphasize on the edges resulted in an abnormally high increase in number of components which suggested low pass filters like Gaussian and Average are more suitable for fMRI preprocessing.

COMPARISON BETWEEN DIFFERENT TECHNIQUES OF PREPROCESSING FOR RESTING STATE fMRI ANALYSIS

by
Megha Girdhar

A Thesis
Submitted to the Faculty of
New Jersey Institute of Technology
in Partial Fulfillment of the Requirements for the Degree of
Master of Science in Biomedical Engineering

Department of Biomedical Engineering

May 2010

Blank Page

APPROVAL PAGE

COMPARISON BETWEEN DIFFERENT TECHNIQUES OF PREPROCESSING FOR RESTING STATE fMRI ANALYSIS

Megha Girdhar

Dr. Bharat B. Biswal, Thesis Co-Advisor   Date
Associate Professor of Radiology, UMDNJ-NJMS

Dr. Tara L. Alvarez, Thesis Co-Advisor   Date
Associate Professor of Biomedical Engineering, NJIT

Dr. Richard A Foulds , Committee Member   Date
Associate Professor of Biomedical Engineering, NJIT

BIOGRAPHICAL SKETCH

Author: Megha Girdhar

Degree: Master of Science

Date: May 2010

Undergraduate and Graduate Education:

- Master of Science,
  New Jersey Institute of Technology, Newark, NJ, 2009

- Bachelor of Engineering
  Prabhu Dyal Memorial College, Bahadurgarh, Haryana, India, 2006

Major: Biomedical Engineering

"This thesis is dedicated to my fiancé, Pradeep Kumar, who encouraged me, and put his academic profession on hold so I could achieve my dream. Thank you, Pradeep, for your love, wisdom and support. To my parents, Harish and Asha Girdhar, your prayers have been answered. Also to my sisters, Bhumika and Neha, and my brother Amar, not a day did you complain about how busy I was. I thank you for your understanding and patience. To my extended family: God has shown it again."

ACKNOWLEDGMENTS

I would like to express my sincere gratitude to my research supervisor, Dr Bharat B. Biswal, for his enormous help and guidance towards this thesis. Thanks are also given to Dr. Tara L. Alvarez, for being my co-advisor and supporting me through this thesis. I deeply appreciate Dr. Richard A. Foulds for actively participating in my committee. I would also like to acknowledge Dr Manjula Khubchandani, and my colleagues; Suril Gohel, and Amit Kamble for making this opportunity at UMDNJ a great learning experience and making every moment count memorable.

TABLE OF CONTENTS

LIST OF FIGURES

LIST OF FIGURES
(Continued)

CHAPTER 1

INTRODUCTION

1.1 Objective

The objective of this dissertation is to investigate various preprocessing techniques and develop optimal methods for analyzing resting state functional Magnetic Resonance Imaging (fMRI) data sets. In this study, different processing steps are performed on the data to differentiate the effects of various processing techniques used on the resting state fMRI data.

To facilitate the comparison of effects between voxels, regions, subjects, or groups using fMRI, a standardized set of preprocessing steps are used for all the subjects. These preprocessing steps include a number of algorithms to reduce noise effects, and to transform the brain into a standardized brain to facilitate direct comparison between corresponding voxels between different subjects (brains). The preprocessing steps further remove variance arising from random physiological events or instrumentation problems and increase signal to noise ratio (SNR) such that the resultant data is suitable for statistical analysis. These preprocessing techniques vary highly according to the requirements and interests of user. All of these requirements make it vital to have the same processing pipeline for fMRI preprocessing.

Resting State Network (RSN) has become a useful tool in medical field to classify various diseased and normal state of brain. Recent studies have suggested that the normal functional connectivity changes in the state of the various brain disorders e.g. depression, Schizophrenia, Alzheimer, multiple sclerosis. Continued research in this field has shown

a potential to predict individualistic responses to specific anti-disease medications based on the patterns of brain network activity as visualized by functional connectivity analyses. The goal of this dissertation is to study the effect of post-processing methods, its effect on connectivity analysis, and to develop an optimum way to process resting state data sets.

1.2 Background Information

In the early 1990's, the development of fMRI equipped clinical research community with a sophisticated tool to measure any activity in the various regions of brains. The regional cerebral blood volume (CBV) was first utilized by Belliveau[1] in 1991 to construct functional magnetic resonance maps of brain. Ogawa et al. [2] coined the term blood oxygen level dependent (BOLD) to measure task induced functional changes in the brain. Both of these techniques were first used to detect visual tasks in the primary visual cortex. It is currently hypothesized that task activation leads to increased neuronal firing which in turn leads to increase in cerebral blood flow in the activated regions in the brain. Thus fMRI task induced signal changes is an indirect measure of neuronal activity. Over the years, fMRI development and implementation has allowed researchers to study and differentiate activated regions of brain.

Other than the above-mentioned task related networks, a low frequency (<0.1 Hz) network was first described by Biswal et al in 1995 [3], in the region of sensorimotor cortex as a state of brain when almost no stimuli are present or applied - better known as resting state network or default network. Later, De luca et. al.[10] described the resting state connectivity as long distance interactions in various distinct regions of the brain

including medial temporal lobe (memory), medial prefrontal cortex (mental stimulation), posterior cingulated cortex (integration), adjacent precuneus and inferior parietal cortex. Recently, Buckner et al.[4] have suggested that default network is a specific region of brain which is active for individual subjects when they are not focused on external environment. Samantha et. al. [5] proposed and described the mechanism for abnormality in resting state network for some mental disorder cases.

While performing various experiments, different preprocessing techniques were developed and applied. Preprocessing of fMRI data is essential to account for motion and noise properties, and was required because number of parameters which were not useful for the purpose, were needed to be suppressed or removed completely from the data for further analysis and to achieve that a number of techniques have been developed and implemented. Many different parameters need to be compared while making a choice to achieve an image with appropriate attributes like signal to noise ratio (SNR), contrast and other information. This information is dependent on the pulse being used for fMRI, the organ being imaged as well as on field strength of the MRI machine. In 1995, Worsley and Friston [6] developed a method for activation by analyzing time series based GLM (general linear model) and a heuristic analysis for the effective degree of freedom. The Importance of spatial smoothing is explained by Triantafyllou [7]. Some high resolution and spatially smoothen images were compared in the study and it was suggested that not all the studies required high resolution images. Similarly, temporal filtering is required to increase the sensitivity and selectivity in event related designs [8]. Various filtering methods have also been compared by Kruggel et.al. [9]. Identifying a proper

preprocessing approach is still an ongoing topic of research as a preprocessing method may be appropriate for one purpose and can be totally inappropriate for other purposes.

This thesis uses fMRI to investigate the extent of spatial and temporal inter-subject synchronization during a complex stimulus using multiple analysis methodologies. Following the background studies described previously in Chapter 1, Chapter 2 presents the fundamentals of functional magnetic resonance imaging including a description of the scientific principles behind the generation of the fMRI signal, biological properties represented in the signal and a brief description of resting state networks. Chapter 3 discusses various methods and approaches followed in this paper. Chapter 4 provides a detailed outline of the investigational study performed for this thesis and a discussion of the results obtained. Chapter 5 concludes the work presented.

CHAPTER 2

BASIC FUNDAMENTALS OF FUNCTIONAL MAGNETIC RESONANCE IMAGING

2.1 Nuclear Magnetic Resonance

Nuclear magnetic resonance (NMR) is the principle on which MRI/fMRI techniques are based. The nuclei of an atom contain unpaired charged electron/protons that spin around their axis in the presence of external magnetic field and produce their own opposing magnetic field. Hydrogen atom, which is most abundant in the human body, is commonly used for this purpose because its nucleus is composed of single proton and spinning is relatively uncomplicated. It behaves like a small magnet and produces the NMR signals. The axis about which the protons spin is known as the longitudinal direction while the plane in which precession occurs is known as the transverse plane.

The basic principle can be explained as: when a spinning particle is placed in a magnetic field of strength B, it absorbs a photon of frequency v (containing energy - hv). This frequency of photonic absorption is different for different molecules and depends upon their gyro-magnetic ratio, γ and is represented as:

$$v = \gamma B \tag{2.1}$$

For the hydrogen atom, the gyro-magnetic ratio, γ is 42.58 MHz/T.

2.2   Basics of fMRI

Magnetic Resonance Imaging (MRI) measures the response of the hydrogen atom (or any other MR visible atoms) present in a strong magnetic field. There are four basic steps involved in obtaining MRI image of subjects. First, an external magnetic field is applied around the subject and the spinning particles present inside the subject experience that magnetic field and align themselves in either the same or exact opposite direction. In the second step a radio frequency (RF) pulse is applied with the frequency same as is resonance frequency of the hydrogen atom. Then, the atoms absorb energy from the resonating field and jump into higher energy state which is anti parallel to the external magnetic field. The third step involves the measurement of radio signal emitted by the hydrogen nuclei while coming back to its lower energy state also called relaxation. The fourth and final step transforms that radio signal into a spatial image using three different gradient coils. The different coils separate the signal in terms of space, frequency and phase results in high resolution anatomical image.

A main magnet is used in MRI which produces an external magnetic field and a small number of the protons get aligned parallel to that external magnetic field, which is lower energy state of protons, some of them align in the anti-parallel direction which is at higher energy state. For fMRI, the strength of the magnetic field used is usually between 1.5 to 4.0 Tesla with greater strengths for research applications. The net magnetization factor becomes M_0 in the direction of external magnetic field i.e. the equilibrium magnetization. Similarly, Mz represents the net magnetic field in Z (vertical) direction after applying the RF signal.

The signal received from MRI pulse sequence needs to be converted into frequency domain for image reconstruction. The conversion is done by using pulse sequences which is defined as set of RF pulses applied to produce specific form of NMR signal. The dual spin echo is shown in the figure below. The pulse sequence timing can be adjusted to give different type of image contrast e.g. T1-weighted and T2-weighted proton density images.
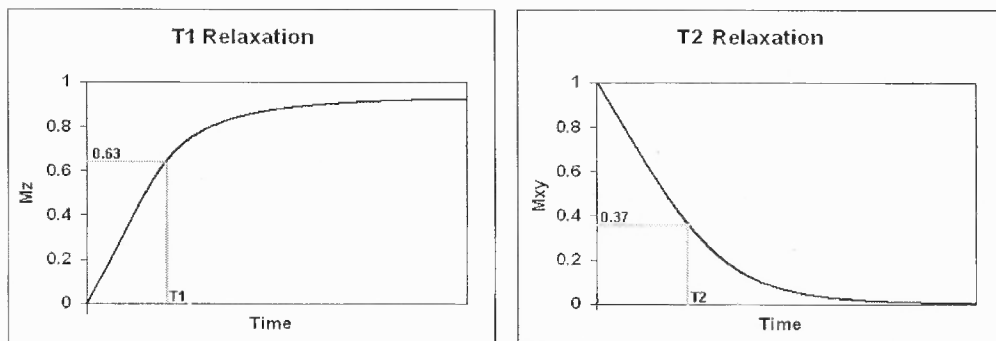
Figure 2.1 T1 and T2 relaxation curves.

Proton density is the concentration of protons in the tissue in the form of water and macromolecules (proteins, fat, etc). The T1 and T2 relaxation times define the way that the protons revert back to their resting states after the initial RF pulse. In case of 90' pulse, the T1 relaxation is time during which the longitudinal magnetization returns back from zero to maximum amplitude. Whereas, T2 relaxation is the time which the transverse magnetization returns back to zero from maximum. The both terms are independent. T2 relaxation generally occurs faster than T1 relaxation. The rephasing of the spins can be explained using the Equation 2.2.

$$M_z(t) = M_0(1 - e^{-t/T1})$$ (2.2)

Where, $M_z(t)$ is longitudinal magnetization at any time t and T1 is decay constant of the magnet (time required to reach 63% of maximum M_z).

T1 relaxation varies with tissue properties. Very small molecules rotate very quickly and thus they give very less potential of resonant frequencies while large molecules rotate slowly and do not give any useful resonant frequency. Since studies have shown that T2-weighted images are most sensitive for detecting brain pathology. Therefore, T2-weighted images are used for fMRI imaging.

2.3   Functional MRI

Advancement in MRI has led us to the development of fMRI (functional Magnetic Resonance Imagining). Unlike MRI, fMRI not only gives the high resolution anatomical images of the brain it also provides high temporal resolution. fMRI measures the confined changes in the cerebral blood flow in terms of its volume and oxygenation. fMRI has made it feasible to localize different regions activated during particular tasks performed at that specific time. The basis of most fMRI techniques uses BOLD (Blood oxygen level dependent) principle. Figure 2.2 shows a schematic representation of the BOLD mechanism. The increase in brain activity requires more oxygen intake which is linked with more blood flow. The amount of oxyhemoglobin increases and deoxyhemoglobin decreases. The paramagnetic properties of deoxygenated hemoglobin produce the inhomogeneous magnetic field resulting in low intensity T2* weighted image. Changes in BOLD signal measured against time, also known as hemodynamic

response function (HRF), provide information on brain activity. The fMRI response when compared with other cognitive techniques is found to be superior in terms of spatial resolution. The temporal resolution however is not in the millisecond range but more in the second range, but the combined results give very meaningful information which has not been achieved by any other techniques developed so far.
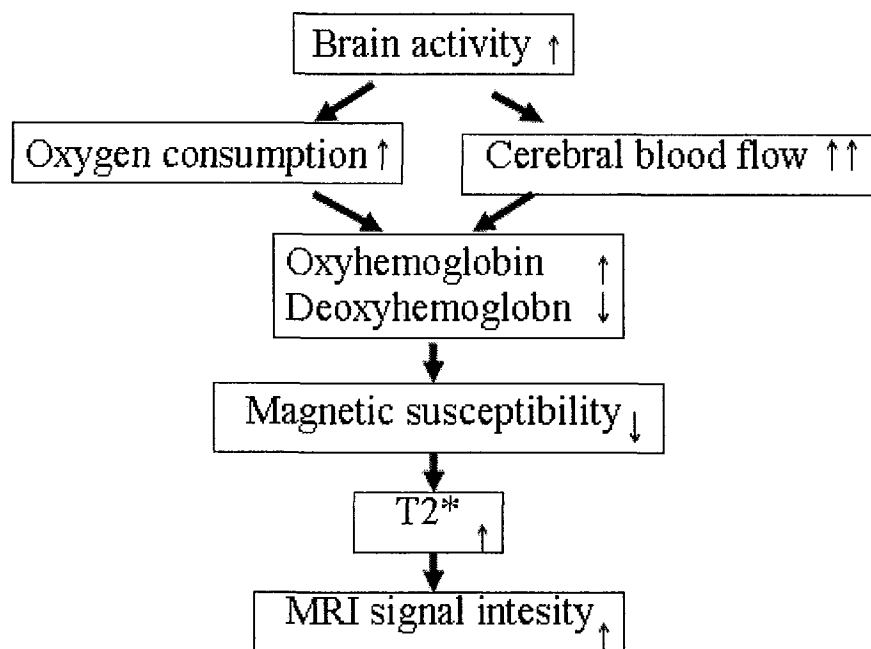
Figure 2.2 Mechanism of BOLD signal.

During task related fMRI measurement, blood-oxygen levels change in the brain in eloquent regions due to increased neural activity. This allows measurement of brain activity that has a sensitivity of seconds in time and millimeters in space. Also, fMRI being non-invasive can be quickly repeated multiple times if required. All of these advantages have made it one of the most commonly used medical imaging tool to study the brain activity for both clinical and research purposes.

2.4   fMRI Analysis

Although the brain is continuously active implying that the blood oxygenation level varies continuously in the brain irrespective of the absence or presence of any specified task, it is currently believed that even during the presence of tasks, task induced signal changes account for only about 7% of this variation, the rest 93% accounts for the baseline (rest) activity changes in the brain Therefore, it is important to maintain same exact experimental conditions while conducting fMRI experiments. During an experiment, MRI scanner usually covers the entire volume of brain in about 2-4 seconds and 100s of such brain volumes are sequentially collected. Prior to generating activation map representing functional regions corresponding to the stimulus presented, several preprocessing steps are required to be performed.

- Slice time Correction: the time gap between different slices is kept uniform

- Motion Correction: minimizes the effects of motion in the data

- Spatial Smoothing: reduces effects of high frequency components

- Temporal Filtering: to remove variation due to heart beat and respiration

- Normalization: to convert images in standard MNI space

2.4.1   Slice Time Correction

fMRI technique is highly dependent on the sequence of images collected during each volume acquisition.. Therefore, it is important for all time series to be synchronized. Slice time correction makes an account of time difference between the slices. Slices are often acquired in an interleaved manner, sometimes increasing the time-difference between two

slices to TR/2. Slice time correction is achieved by interpolating time series of each voxel with a fixed reference.

2.4.2 Motion Correction

While mapping the brain activity using fMRI one of the most common factors adversely affecting the processing is the motion of the subject during the data-acquisition process. As the time of scanning varies from 4-5 minutes it is difficult to stay steady even motivational subject move substantially. As a result of this, time series obtained would be affected with loss of signal or the signal mixing up with other regions and hence resulting into errors. Therefore, it is very important to identify if there is any motion and rectify it before proceeding with any further step in data analyses.

2.4.3 Spatial Smoothing

The noise present in each image is minimized using spatial smoothing. In fMRI, Spatial smoothing improves the ability statically interpolations to detect activation by increasing the signal-to-noise ratio (SNR) but at the same time it reduces the spatial resolution. Therefore, it is important to maintain the balance between SNR and image spatial resolution while performing spatial smoothing. The spatial smoothing is typically accomplished using various filtering kernels including Gaussian, Average and Hamming.

2.4.4 Temporal Filtering

The purpose of fMRI data is to identify the changes in the temporal brain signal intensity changes. The time series contains all important information of brain activity. But usually the time series are contaminated by the noise present during the experiment which could be due to the other tasks being performed by the subject simultaneously or because of

some technical problem. To get rid of this unwanted signal temporal filtering is required. For this purpose, usually a band pass filter is used which attenuates the unwanted frequency contents of signal.

2.4.5 Normalization

To account for variation in the brain structures among different subjects, each individual brain is typically transformed into a standardized brain template. Technical interpretations of results are facilitated by comparing fMRI images of the brain visually or by some statistical analysis for different data sets obtained from different facilities across the globe. Quantitative analysis requires the alignment of images before making any interpretations. So it is required to convert all the brain images into a standard space, Montreal Neurological Institute (MNI) approach is most commonly used for that purpose.

2.5   Statistical Analysis

The statistical analysis is performed on the pre-processed data to interpret data and obtain robust results. Several ways to interpolate the results have been proposed which allow identifying the region of interest in brain. These regions usually show significant correlation with the task performed – giving a meaning to the whole process.

2.6   Resting State Connectivity

The brain during rest activates a number networks including the default mode network. This is the activation recorded when the subject is doing nothing but resting. It is presumed to be described by coherent neuronal oscillations of frequency range less than

0.1 Hz. It has been observed that during the task related networks, the resting state network is usually deactivated and it is activated during day dreaming, retrieving memories, and gauging others' perspective. The medial temporal lobe for the memory, part of the medial prefrontal cortex, the posterior cingulated cortex with adjacent precuneus and media, and the lateral and inferior cortex are the regions of the brain that are supposed to cover the resting state network [10]. As shown in figure 2.3, De luca et. al.[10] described the resting state connectivity as long distance interactions in various distinct regions of brain including medial temporal lobe (memory), medial prefrontal cortex (mental stimulation), posterior cingulated cortex (integration), adjacent precuneus and inferior parietal cortex.

The increasing interest in resting state network in both clinical and basic science research community is due to its capability to indicate distinct changes in inter-regional functional connection strength in case of any dysfunction in the brain activity. Few of the examples where the resting state networks have been applied to diagnose "illness" in clinical sciences are:

- In multiple sclerosis low frequency BOLD fluctuations were observed in bilateral primary motor cortices.

- In identifying, early Alzheimer's disease to the hippocampus and between posterior cingulate cortex and hippocampus.

- Within the cortico-limbic network in depression. Also increased contributions from subgenual cingulated cortex and thalamus in depressive patients.

- In schizophrenia patients, altered resting state connectivity of the hippocampus has been reported.

There are many possible applications of resting state networks in clinical sciences. Its various utilities suggest that RSN can serve as an indicator in many dysfunction of brain connectivity. Therefore, it can be used as biomarker for a number of diseases.
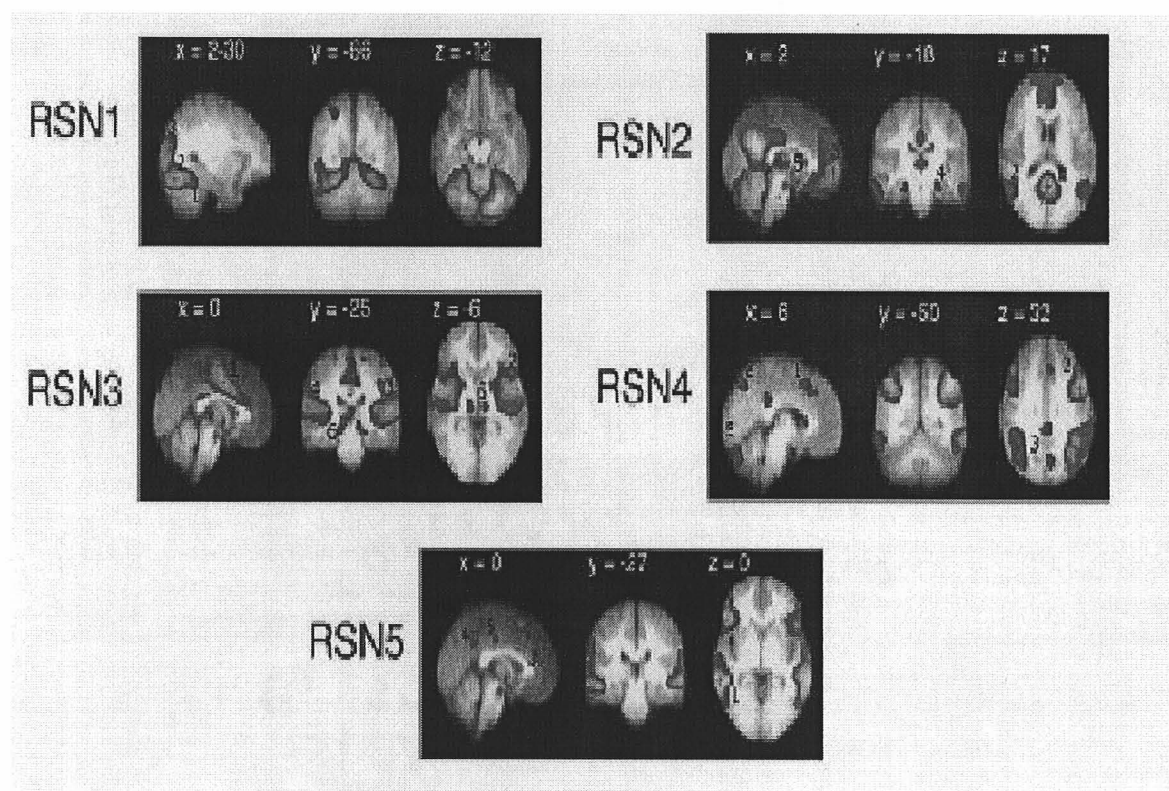

Figure 2.3 The five distinct regions are describes as five resting state network in the brain by De Luca et al[10]

2.7   Independent Component Analysis (ICA)

ICA is a statistical and computational method for revealing hidden factors that underlie sets of random variables, measurements, or signals. It was first introduced in early 1980s

which was related to neural network modeling. After that, in 90s its improved version with successful algorithm was demonstrated on problems like cocktail-party effect, where individual speech waveforms were separated from their mixed-up signal.

ICA helps in solving the problems with linear and nonlinear mixture of unknown variables. The latent variables are assumed to be independent and non-Gaussian.

ICA is also commonly known as blind source separation technique. Typical examples of ICA problem are where, a mixture of simultaneous speech signals has been picked up by several microphones, brain waves recorded by multiple sensors, interfering radio signals arriving at a mobile phone, or parallel time series obtained from some industrial process. Now ICA is known as a popular tool in the field of neural networks, especially unsupervised learning, and more generally in advanced statistics and signal.

To rigorously define ICA, we can use a statistical "latent variables" model. The n random variables x_1, x_2, x_3...............x_n, are observed which are modeled as linear distribution of n random variables s_1,s_2,s_3,s_4............s_n.

$$X_i = a_{i1}s_1 + a_{i2}s_2 + a_{i3}s_3 + a_{i4}s_4 + ... + a_{in}s_n$$

For all i=1,...................,n . Where the $a_{ij}, i,j = 1,.......,n$ are some real coefficients. By definition, the s_i are statistically mutually independent.

This is the basic ICA model in which observed data are generated by mixing the components sj, therefore it is known as generative model. The independent component sj are latent variable which cannot be observed directly. Also the coefficients a_{ij} is assumed

to be unknown. All we observe are random variables xi, and we estimate both a_{ij} and

s_i(ICs) using only x_i. For that we must make some general assumptions, like:

- The independent components are assumed to be statistically independent.

- The independent components must have non-Gaussian distributions.

- For simplicity we assume that the unknown mixing matrix is square.

2.8   Probabilistic ICA Model

There are number of techniques available to calculate Independent Components for

fMRI. The PICA (probabilistic independent component analysis) is one of them. This

technique was optimized for the analysis of fMRI data by Beckman and Smith [16] and

later the role PICA for investing resting state networks was implemented by Beckmen et

al. [15] to characterize the spatiotemporal structure of resting state data. A probabilistic

ICA extends the ICA model by assuming that the p-dimensional vectors of observations

(time series in the case of FMRI data) are generated from a set of q(< p) statistically

independent non-Gaussian sources (spatial maps) via a linear and instantaneous 'mixing'

process corrupted by additive Gaussian noise

$$\eta(t): x_i = As_i + \eta_i$$

Here, x_i denote the individual measurements at voxel location i, s_i denotes the

non-Gaussian source signals contained in the data and η_i denotes Gaussian noise $\eta_i \sim$

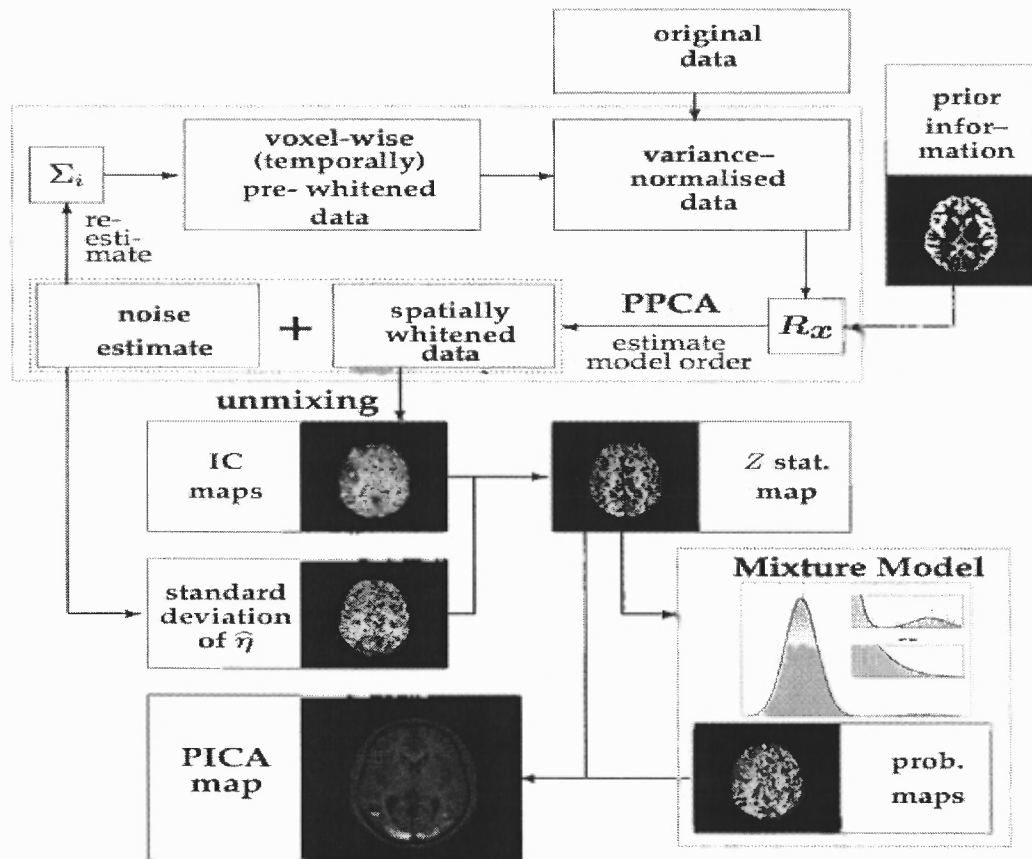$G(0, \sigma^2 \Sigma_i)$. Following Figure 2.4 captures all the individual steps applied for PICA.

Figure 2.4 Flow chart of the analysis steps involved in estimating the PICA model (Beckmann and Smith (2004)

CHAPTER 3

METHODS

3.1 Data Acquisition

For the purpose of this resting state fMRI preprocessing study, the data was collected from the multisite human connectivity study, freely available at www.nitrc.org. All the data used for this study was collected at the Massachusetts Institute of Technology (MIT). In this experiment, 39 healthy subjects with no prior history of any neurological and psychological diseases were involved. All subjects were healthy adult between the ages of 21 to 50 years. Two scans of each subject were taken. One of these was high resolution anatomical image called MPRAGE image and other scan was taken when the subjects were resting. At the time of rest-scans, the subjects were instructed to keep their eyes closed and they were asked to refrain from performing any cognitive or motor activity.

3.2 Data Analysis

A number of methods have been used to provide functional connectivity estimates for an fMRI dataset. Choosing appropriate preprocessing parameters is very important from the perspective of functional connectivity estimation, since it determines the significance of the fMRI signals. Different software were used for preprocessing this study including AFNI, FSL and MATLAB. A Perl script incorporating the various command lines using AFNI and FSL was also developed for this purpose.

Different methods of doing motion correction, temporal and spatial smoothing involving a number of steps were performed to see the effect of each step independently on processing the data, and then the results from these methods were compared. The preprocessing methods investigated in this study are described below.

3.2.1 De-oblique

The functional scan consists of a number of slices in sequence through the entire volume of brain. In this experiment, data were acquired in oblique/angled manner as shown in the figure below. The advantage of the oblique scan is that it avoids the air-filled sinuses present in front of the head otherwise this air interferes with MR signal, resulting in poor quality of image. Because any form of signal loss will adversely affect the data, oblique slice are used to minimize these effects. In this study, the dataset is first de-obliqued to proceed further.
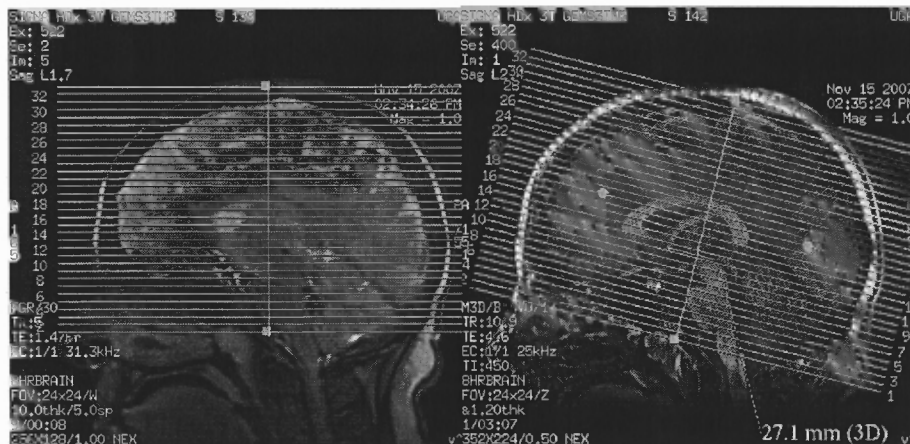

Figure 3.1 Two different ways of slice acquisition (in the left image (a) the slices are obtained in an axial manner parallel to transverse plane and (b) the slices are acquired in an oblique manner with an angle of around 30 degrees with transverse plane).
(source: http://ccnlab.myweb.uga.edu/afniwiki/fmri.html)

3.2.2 Slice Time Correction

While scanning different slices of the brain usually a time lag occurs between scanning of different slices. This time lag depends on the acquisition setup. Slices are acquired in a straight or interleaved sequence i.e. even number slices are acquired first and then the odd numbered slices. In interleaved sequence the probability of the time lag between acquiring data for each slice will cause the difference in the signal which can be substantial mainly in the studies related to even number slices. Although it doesn't affect the individual voxel analysis but future processing steps like spatial smoothing, motion correction, temporal filtering and normalization may be affected. Therefore, it is important to correct for this time lag and 3dTshift function in AFNI is used for such slice time correction. 3dTshift can also be used during motion correction with 3dvolreg.

3.2.3 Motion Correction

Motion correction was performed to remove the effect of subject movement during the experiment, which is considered as one of the main source of data loss in fMRI. 3dvolreg in AFNI was used for the purpose of correcting data for any such motion. Many different options are available in AFNI for motion alignment apart from 3dvolreg. 3dvolreg has been proved to be accurate and more computationally efficient [17]. 3dvolreg, based on least square objective function, is a very fast method for rotating and aligning images. Different options available for 3dvolreg are Fourier, Cubic, Quintic, Heptic and Clipit. These are the different algorithms for motion interpolations where Cubic refers as polynomial fit of third degree, Quintic refers to polynomial fit of fifth degree and Heptic refers to polynomial fit of seventh degree. Fourier as proposed by Eddy et al. [18], is a

special method where the data points are equally distributed and then correction is done by discrete Fourier transform. In the Clipit method, as the input volumes might produce values outside the input range, the program clips the value in each out-brick into the same range. The example of command line used for Motion Correction.

3dvolreg –fourier (cubic, heptic, quintic, clipit) –base dataset[5] -prefix outputname

Here, 3dvolreg is the AFNI command, Fourier is the type of interpolation opted where Cubic, Heptic, Quintic, Clipit can also be used. Base is the reference point where interpolation is done and then prefix specifies the output name.

3.2.4   Spatial Smoothing

Spatial Smoothing is required to increase the signal to noise ratio by removing unwanted information from the signal. Spatial smoothing on the images is performed in the image space. Attenuating high frequency results in a smoother image where low frequencies emphasize on the contrast and result in enhanced edges for images. A number of different frequency filters can be used for spatial filtering. In AFNI, spatial smoothing is done by using 3dmerge command opting from many available parameters. The different values of full width at half maximum (FWHM) of 4, 6 and 8mm were applied and results obtained were compared. MATLAB also provides ability to spatially smoothen the data. Four different types of MATLAB filters were tried for spatial smoothing using 2D filter (filter2) by changing the type in FSPECIAL (type) between Gaussian, Average, Unsharp and Sobel.

3.2.4.1 Gaussian Filter Gaussian is a 2D smoothing filter operator which blurs the image and minimizes the noise. Although the operation is similar to that of Average filter but the shape of Gaussian kernel is different and in 2D, it is represented by

$$G(x,y) = \frac{1}{2\pi\sigma^2}e^{-\frac{x^2+y^2}{2\sigma^2}}$$

Where σ is standard deviation, and it is assumed that the mean of function is zero for the equation above i.e. center lies at zero. 3D representation of this function is shown in figure below.
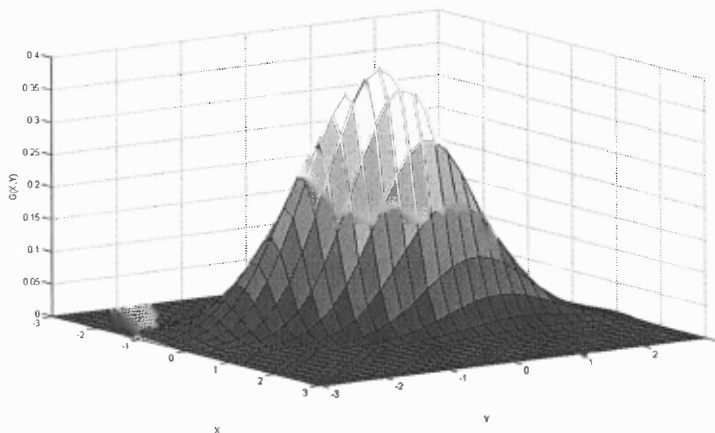

Figure 3.2 3-D representation of gausian function

This 2D distribution as point spread function is used by convolution in Gaussian smoothing. Image is stored in a matrix with distinct values for all pixels. In the similar way a matrix of Gaussian function is generated using convolution matrix as shown in figure 3.3. In MATLAB, FSPECIAL('gaussian', N, σ) returns a rotationally symmetric Gaussian lowpass filter output with standard deviation σ, where σ is measured in pixels.

N is a vector specifying the number of rows and columns. The default parameters for N
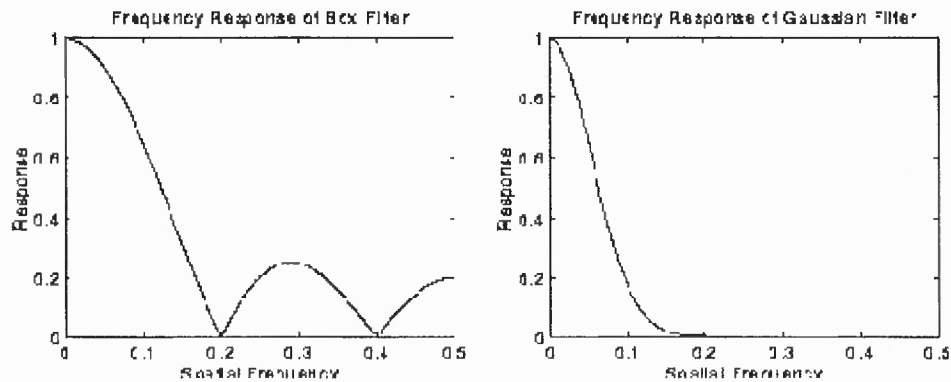and σ are [3 3] and 0.5.

Figure 3.3 Frequency responses of Gaussian and Average filters
(source: http://homepages.inf.ed.ac.uk/rbf/HIPR2/gsmooth.htm)

$$\frac{1}{273}$$

1	4	7	4	1
4	16	26	16	4
7	26	41	26	7
4	16	26	16	4
1	4	7	4	1

Figure 3.4 Matrix representation of a Gaussian function

3.2.4.2 Average Filter This filter is simple and can be efficiently implemented. It
reduces noise in the images by reducing the intensity variation between adjacent pixels.
It replaces intensity of each of the pixels with the mean value of its adjacent neighboring
pixels. FSPECIAL ('average', N) returns an averaging filter applied to the signal where
default value of N is [3 3]. Matrix sizes [5 5] and [7 7] were also tried for this study. The
[3 3] matrix used for Average filter looks as shown in the table below.

$\dfrac{1}{9}$	$\dfrac{1}{9}$	$\dfrac{1}{9}$
$\dfrac{1}{9}$	$\dfrac{1}{9}$	$\dfrac{1}{9}$
$\dfrac{1}{9}$	$\dfrac{1}{9}$	$\dfrac{1}{9}$

Figure 3.5 Matrix for Average function

3.2.4.3 Unsharp Filter Unsharp filter is also simple and works as high pass filter. It enhances the edges and other high frequency components in the image by subtracting the Unsharp or smoothen components from the image.

FSPECIAL('unsharp', α) returns a 3-by-3 Unsharp contrast enhancement filter applied to the signal. The Unsharp filter is created from the negative of the Laplacian filter with parameter α where α controls the shape of the filter and ranges between 0 to1. Default value of α in MATLAB is 0.2.

3.2.4.4 Sobel Filter FSPECIAL('Sobel') returns a 3-by-3 filter that emphasizes on horizontal edge. The smoothing is done by approximating vertical gradient. The vector matrix is [1 2 1; 0 0 0; -1 -2 -1;].

3.2.5   Temporal filtering

fMRI measures the activity of the brain by scanning the regions of brain for a particular period of time with a specific sampling rate which is represented by its time series. Sampling rate or TR (repetition time) of the data was once per two seconds. Each pixel on the scanned image has an independent time series which eventually predicts the changes in intensity of the signal due to hemodynamic response of that region during that

specific period of time. This time series not only contains the required information of brain activity but also captures noise of the system.

A band-pass filter for filtering different frequency ranges was used and then compared to optimize range for filtering the data. The background and history of the Resting State Networks suggests that the low frequency components present in the networks are around 0.01 -0.1Hz. In this study, different bandwidths were chosen for this optimization, which were bandwidths of 0.009-0.08Hz, 0.009-0.10 Hz, 0.009-0.12 Hz, 0.009-0.14 Hz and 0.009-0.16 Hz. The filtering is done in MATLAB using band-pass filters of above frequency ranges. The data is of finite length with 150 time samples. Therefore finite impulse response function is applied (FIR). The MATLAB filtfilt function is used for filtering the data. Also, the effect of different windows has been compared by experiment with three those are Gaussian, Rectangular and Hamming.

3.2.5.1 Rectangular Rectangular window is also known as Block window or Dirichlet window. Its shape is like a rectangle which possesses unity gain, i.e. W(n) = 1. Figure 3.6 shown below describes the window used in the MATLAB with order 10. The side-lobe attenuation is given by -13dB and leakage is estimated to be 9.23%.

3.2.5.2 Hamming The Hamming window was initially developed and proposed by Richard W. Hamming. It is the default window for MATLAB function and looks similar to a cosine function. The height of the side lobe is about one- fifth that of the Hanning window and the gain is given by

$$W(n) = 0.54 - 0.46 \cos(2n\pi/N - 1)$$

The MATLAB implementation of Hamming window used in this study is shown below in figure 3.7. It is 10th order window with side-lobe attenuation of -36.7 dB and leakage 0.04 %.
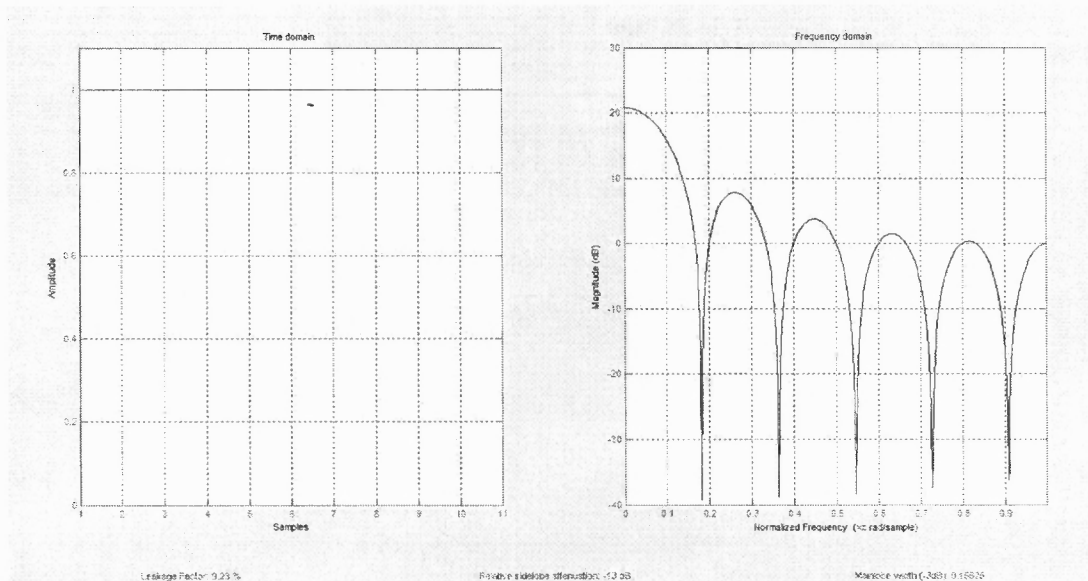

Figure 3.6 shape of the Rectangular window used for temporal filtering in time and frequency domain

3.2.5.3 Gaussian The gain of Gaussian window is given by

$$W(n) = e^{-1/2((n-(N-1)/2)/2)/\sigma(N-1)/2)2}$$

where σ is the standard deviation. The advantage of using Gaussian window for time-frequency analysis is that Fourier transform and the derivative of Gaussian function both are Gaussian functions. For the purpose of this study, a Gaussian window of order 10 was considered. Figure 3.8 below shows the time and frequency domain of the

Gaussian window implemented in MATLAB where sidelobe attenuation is -48 dB and leakage is 0%.
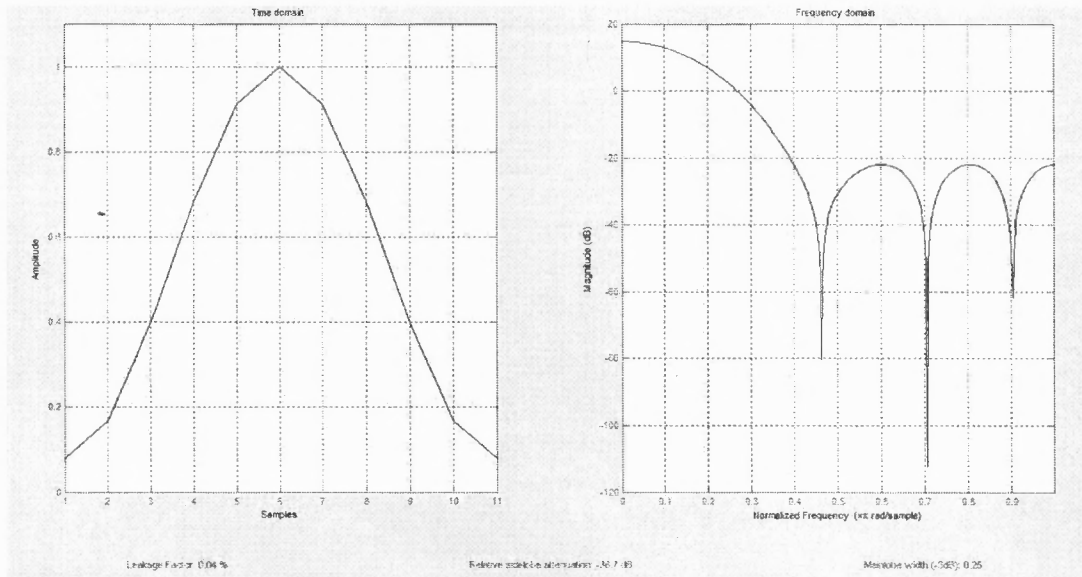

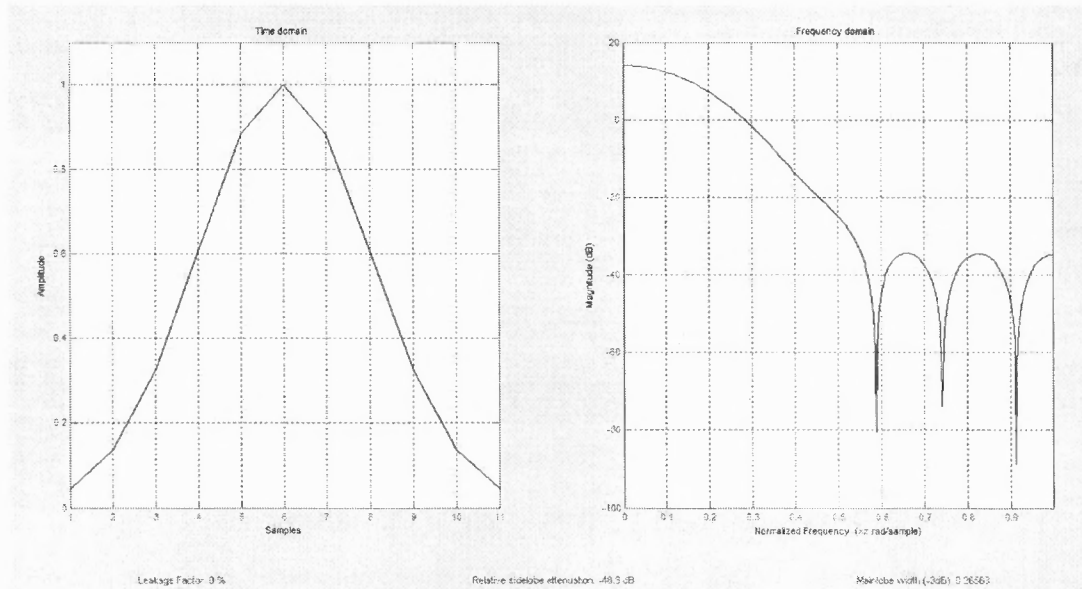**Figure 3.7** shape of the Hamming window used for temporal filtering in time and frequency domain

Figure 3.8 shape of the Gaussian window used for temporal filtering in time and frequency domain

3.2.6 Normalization/Standardization

Normalization in fMRI preprocessing refers to converting the data into standard MNI standard space. Since the data was collected from different subjects in the experiment and the size and the shape of the brain of each subject are different. Therefore, it was required to convert all the information into one standard space before making any crucial interpretations. Normalization was done with the help of *flirt* command in FSL software. The normalization preprocessing was a four step process. In the first step, high resolution anatomical images (mprage) are used to obtain a transformation matrix for given reference image avg12T1_brain.nii.gz. The line below is an example of command used for this purpose where mprage is the anatomical image and input_mni1 is obtained from mprage.

```
`flirt -in mprage.nii.gz -ref avg152T1_brain.nii.gz -omat "$input"_mni1.mat `;
```

In the second step, another transformation matrix is obtained using a reference of mprage in the command line. In the third step, both of these transformation matrices were concatenated and used as input for the last and final step where actual input is converted into MNI space using standard reference image. Here input.nii.gz is the resting state data set, converted into NIFTI format and input_mni2 is another matrix from functional data-set when mprage is used as reference. Following is an example code for this process

```
`flirt -in "$input".nii.gz -ref mprage.nii.gz -omat "$input"_mni2.mat `;

`convert_xfm      -concat      "$input"_mni1.mat      -omat      "$inputto"_mni.mat
"$input"_mni2.mat`;

`flirt -in "$input".nii.gz -ref avg152T1_brain.nii.gz -out "$input"_mni -applyxfm -init
"$input"_mni.mat -interp trilinear`;
```

3.2.7 ICA (Independent Component Analysis)

Independent Component Analysis (ICA) is an important method used to decompose large fMRI data sets into a set of robust connectivity maps. To perform ICA for normalized data, data was first re-sampled into 3mm resolution using 3dresample. The re-sampling was required as the original data had a resolution of 2mm. It takes less processing time for the images with resolution of 3mm than for the images with resolution of 2mm. ICA was performed in FSL using Melodic command where the input type should be in NIFTI. Therefore it was required that data be first converted into NIFTI from AFNI, which was done using command-line 3dAFNItoNIFTI. Also some of the subjects were realigned in RPI using 3dresample.

FSL Melodic ICA is based on PICA (Probabilistic Independent Component Analysis) approach. The data is sent to Independent Component module (called MELODIC, version 3.05) of FMRIB's Software Library (FSL, www.fmrib.ox.a.c.uk./fsl) for PICA analysis. For which, the assumption is made that fMRI signal(x) is generated from linear mixing process of the independent non-Gaussian source (s) and a matrix A. Gaussian noise function (η) is also added to the signal, i.e.

$$x = As + \eta$$

Where, x is a matrix of $p \times n$ dimensions, p is one for this study as ICA is done on individual subjects, n is the number of voxels for fMRI-database and s is $q \times n$ matrix where q is the number of independent components (ICs) which is assumed to be originated from non-Gaussian sources. A is a $p \times q$ mixing matrix and η is simulated

Gaussian noise. Laplace approximation estimation is used to estimate q (ICs). Next, the data-set is reduced to q dimensions and converted into independent components by fastICA algorithm. The matrix W was found to generate a good approximation to the sources, $\hat{S}$.
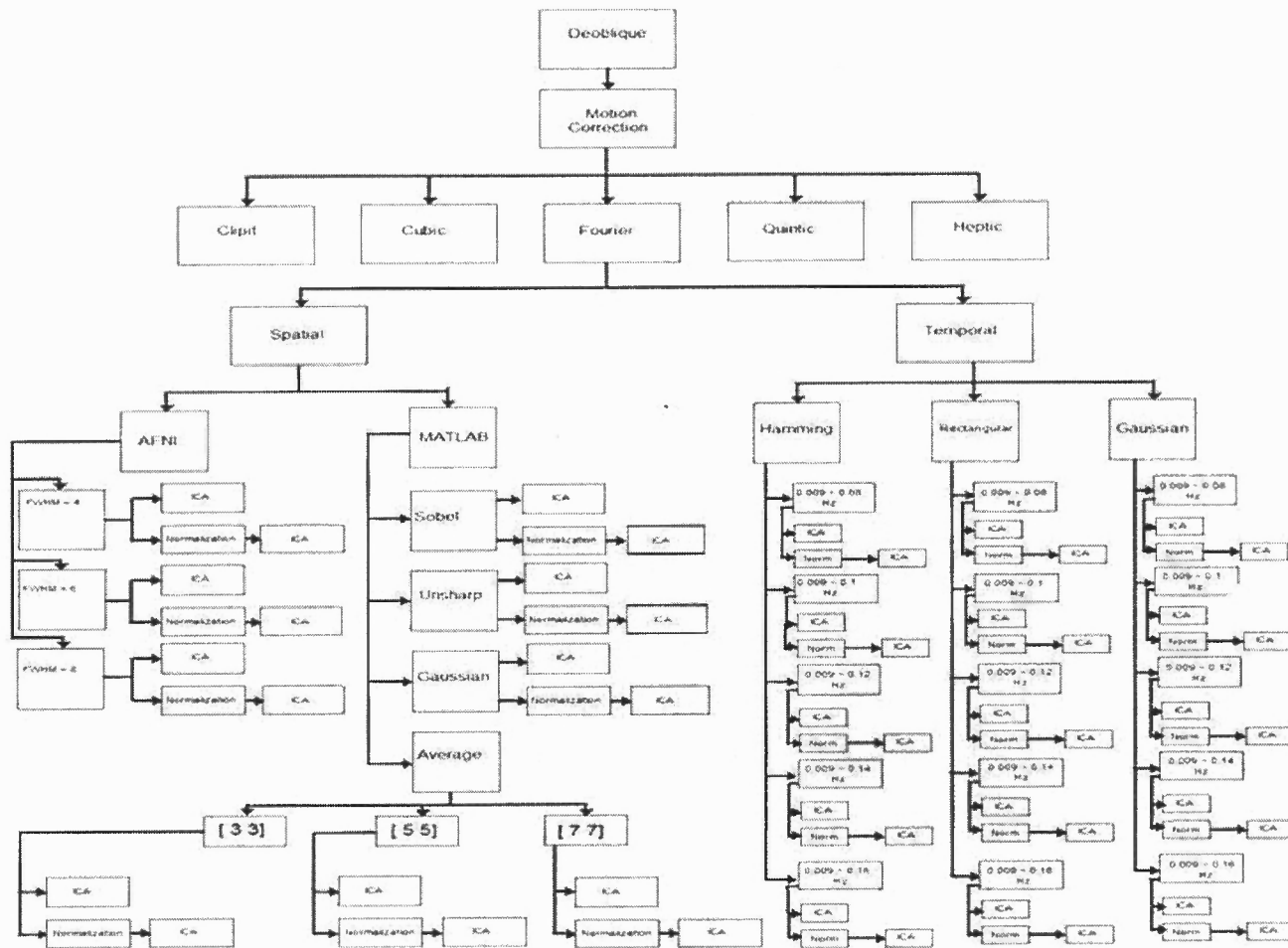
$$\hat{S} = Wx$$

Figure 3.9 Organizational chart of all the steps performed in this study

CHAPTER 4

RESULTS AND DISCUSSIONS

All of the above mentioned methods of preprocessing were tried on the resting state subject-datasets, to find the effect of different preprocessing methods on the resting state fMRI data sets. Also, the same data was converted into MNI space (normalized), preprocessed using same preprocessing methods and then the results were compared with those from previous non-normalized preprocessing.

4.1   Results

4.1.1   De-oblique

Number of components from ICA after de-oblique process were found to be less than those in the original oblique rest data as shown in the figure 4.1 below. Here, the blue curve represents number of ICA components for each subject in original oblique rest data and red curve represents for de-oblique data after using 3dwarp –deoblique.
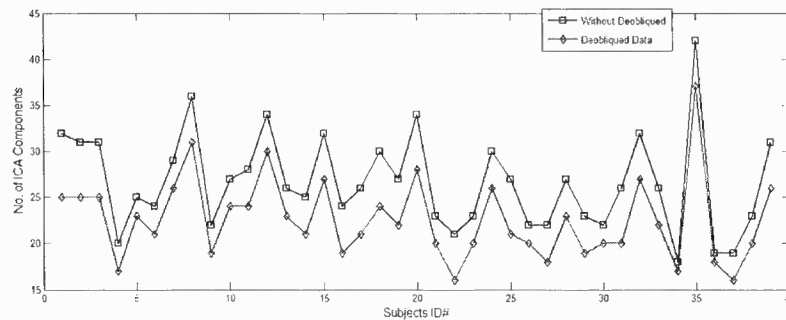

Figure 4.1 The number of ICA components for each subject before and after de-oblique.

32

4.1.2 Slice Time Correction

No time shift was noticed in the given data-set because the data was pre-aligned which was confirmed by application of 3dTshift in AFNI, as it did not suggest any changes to our data-set.

4.1.3 Motion Correction

In each of the studies for motion correction, no significant difference in the number of estimated ICA components was found. Number of ICA components using different motion correction algorithms was observed to be almost same. Also when compared the dataset without any motion correction, the number of components were nearly identical. It can be seen from the curve in figure 4.1 that different algorithms of motion correction using 3dvolreg i.e. Fourier, Cubic, Heptic, Quintic and Clipit, did not have any significant effect
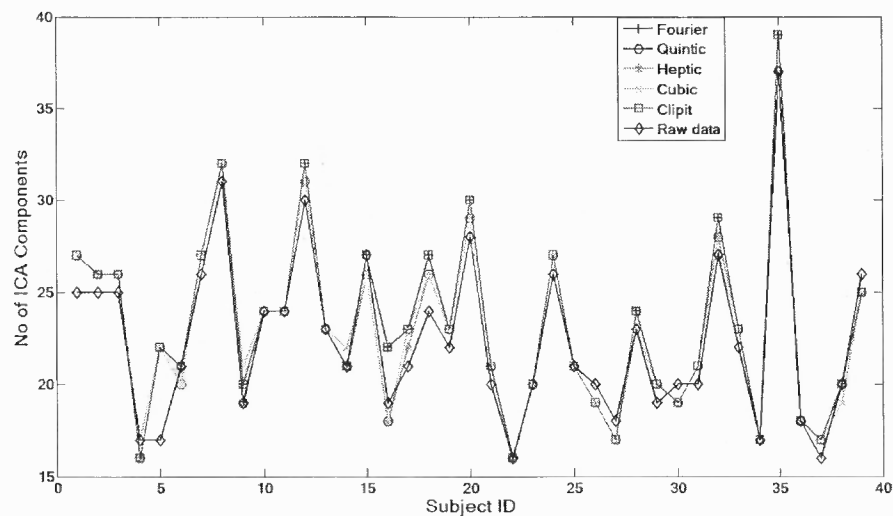

Figure 4.2 Number of ICA components for each subject after motion correction

as the images did not have to be smoothed and realigned because the motion during the scanning was minimal.

4.1.4 Temporal Filtering

As described in methodology section, the data set was filtered temporally using different band pass frequency ranges, to determine the optimal frequency cut off range for resting state connectivity. Temporal filtering was performed using different types of window functions, i.e., Gaussian, Average, Rectangular and Hamming. The results from these windows shown in figures 4.2 and 4.3 indicate that the number of ICA components increase with increase in band width from 0.009- 0.08 Hz to 0.009-0.16 Hz for both Gaussian and Hamming functions. Black curve in the figures shows the number of ICA components from unfiltered raw dataset. The number of ICA components in raw data was found to be much less than that derived from temporally filtered dataset, demonstrating the purpose of temporal filtering.

As with Gaussian function, Hamming function also shows increasing number of ICA components with increase in band width from 0.009- 0.08 Hz to 0.009-0.16 Hz. However, three subjects show relatively less number of ICA components (pink curve) for frequency range 0.009-0.16 Hz in Hamming function. On further analysis, it was concluded that this phenomenon was due to respiration. This is discussed later in discussion section. Also, the number of ICA components for the raw data set is lesser than the filtered data
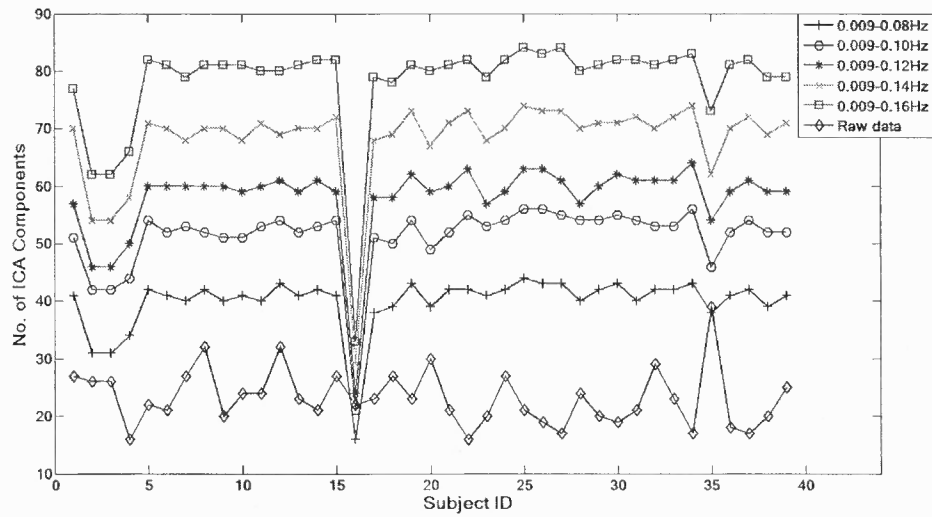
.

Figure 4.3 Number of independent components for each subject from temporal filtering using Gaussian filter. Each curve represents a different frequency range used for band pass filter design.
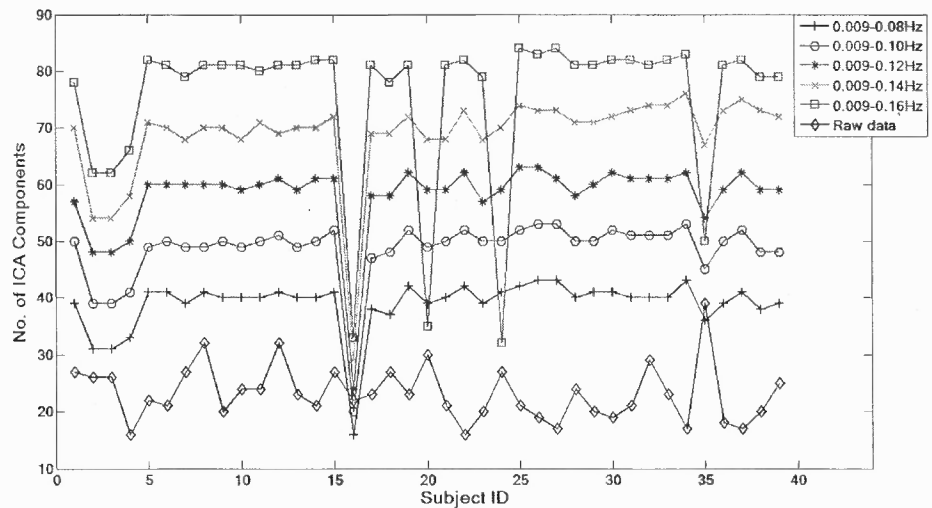

Figure 4.4 Number of independent components for each subject from temporal filtering using Hamming filter. Each curve represents a different frequency range used for band pass filter design.

Figure 4.5 below shows graph for Rectangular window function. However, the trend of increase in number of components with increasing bandwidth was not observed as much as for Gaussian and Hamming functions. This is further discussed later in discussion section 4.2.
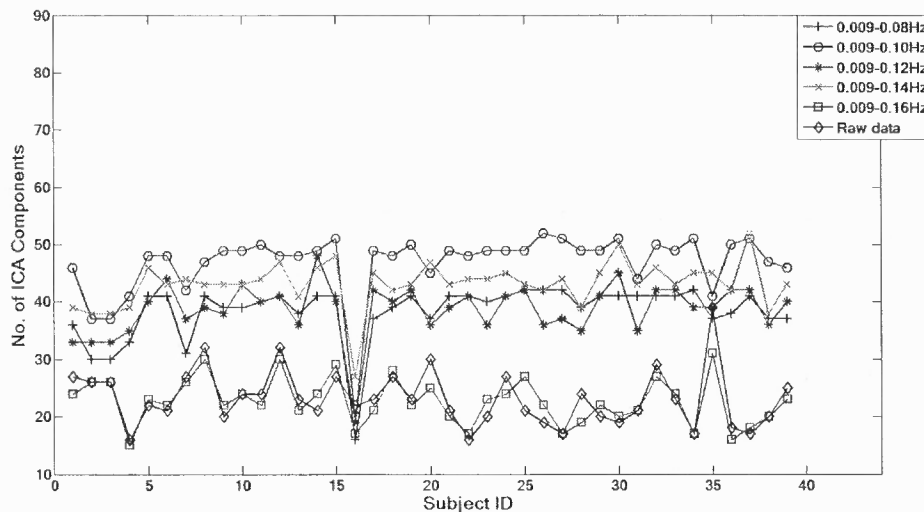

Figure 4.5 Number of independent components for each subject from temporal filtering using Rectangular filter. Each curve represents a different frequency range used for band pass filter design (data-preprocessing was done without converting data into MNI space).

4.1.5 Spatial Smoothing

The dataset was compared for different spatial smoothing methods like Gaussian, Average, Unsharp and Sobel options in MATLAB. Average smoothing method was further tested for different matrix sizes. The results for Gaussian and Average type smoothing are very similar as shown in figure 4.6. Number of ICA components is plotted for individual subjects to compare the type of filters used for spatial smoothing. Here, the Unsharp filter shows slightly higher number of components.
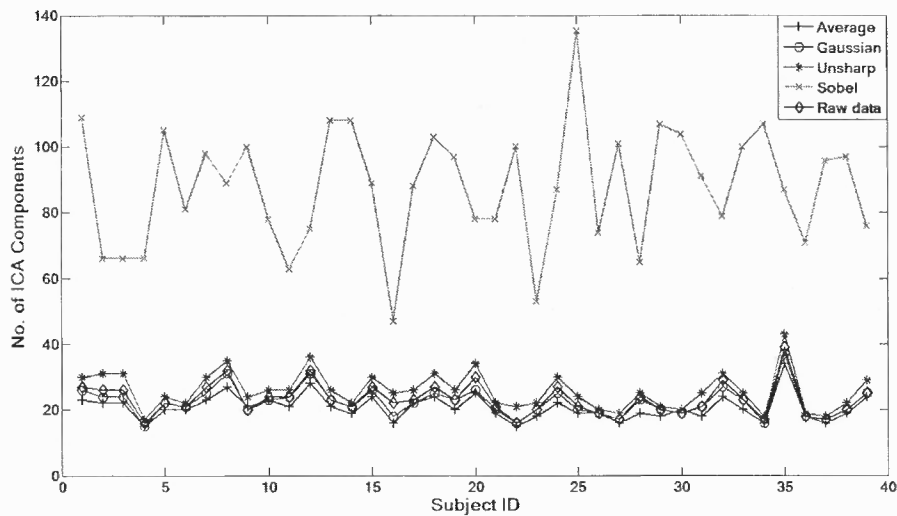
Figure 4.6 Number of independent components for each subject from temporal filtering using Average, Gaussian, Unsharp and Sobel filters. Each curve represents a different frequency range used for band pass filter design (data-preprocessing was done without converting data into MNI space).
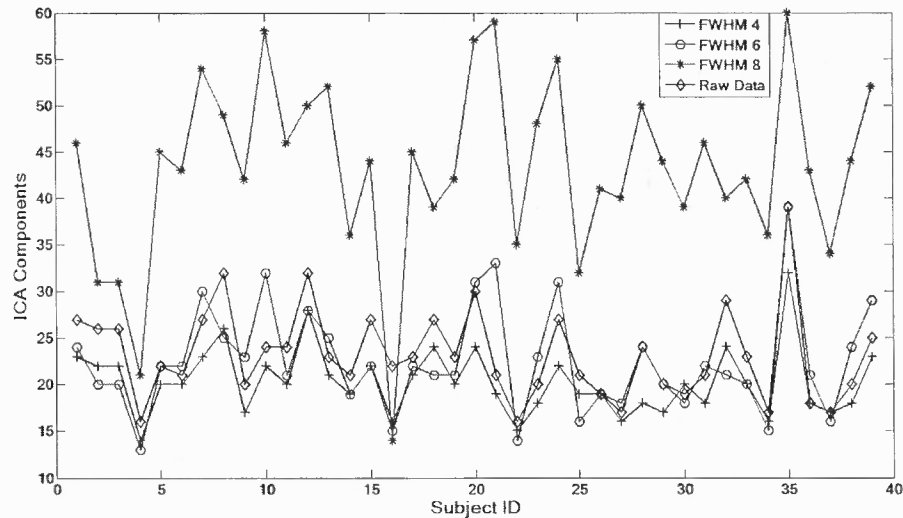

Figure 4.7 Number of independent components for each subject from spatial smoothing in AFNI using different values for FWHM.

In comparison, Sobel filter showed very high number of components for all the subjects. Figure 4.6 shows the spatial smoothing using Gaussian blur filter in AFNI for different FWHM parameters, i.e., 4, 6 and 8 mm. Here, FWHM value of 8mm shows a drastic increase in number of components as compared to 4 and 6 mm. Figure 4.7 shows the graph for number of components for spatial smoothing using Average type filter with different matrix sizes, i.e. [3 3], [5 5] and [7 7].
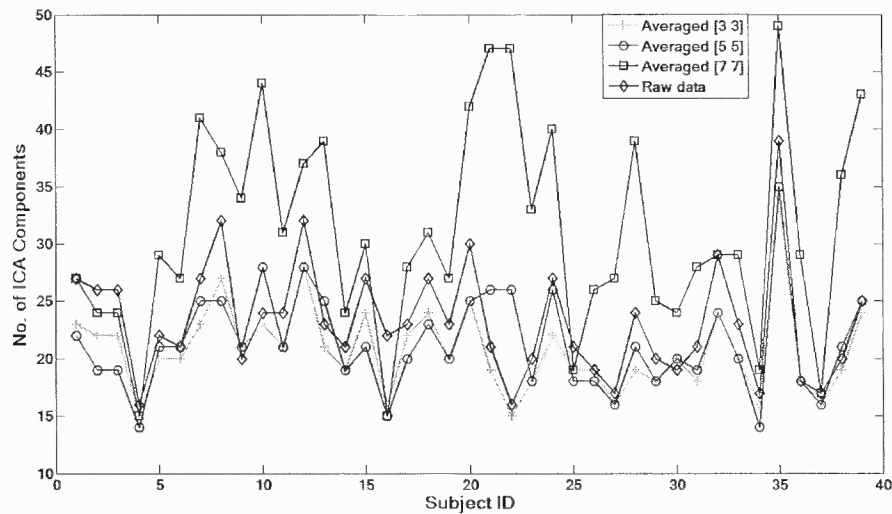

Figure 4.8 Number of independent components for each subject using different matrix size of Average filter.

4.1.6   Normalization

The data-set for which plots and results are presented above, was then normalized to MNI standard brain space before deriving ICA. Numbers of ICA components from this normalized data are plotted in figures 4.8, 4.9, 4.10 using different temporal filtering window functions, i.e., Gaussian, Hamming and Rectangular filters respectively.
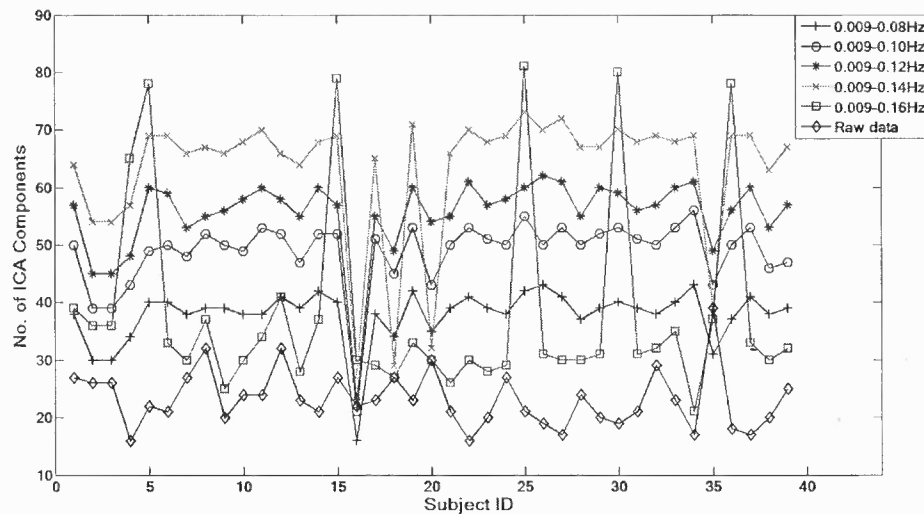
Figure 4.9 Number of independent components for each subject from temporal filtering using Gaussian filter. Each curve represents a different frequency range used for band pass filter design (ICA data-preprocessing was done after converting data into MNI space).

Figure 4.10 Number of independent components for each subject from temporal filtering using Hamming filter. Each curve represents a different frequency range used for band pass filter design (ICA data-preprocessing was done after converting data into MNI space).
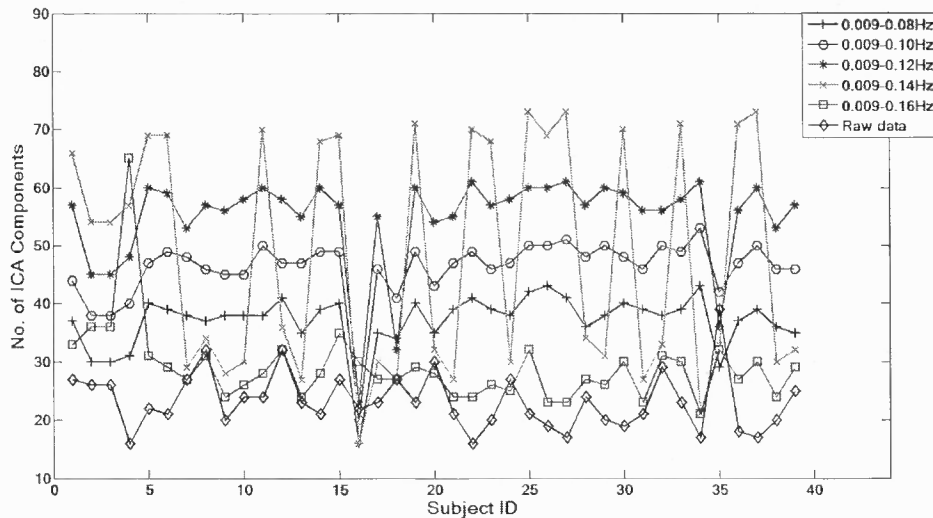
The pattern of ICA components for different filter bandwidth observed with non-normalized data as described previously was different for data converted in the standard

brain MNI space. In the case where dataset was normalized to standard brain space, the number of ICA components increased until the bandwidth of (0.009-0.12) Hz and then started decreasing instead of continuously increasing for all bandwidths of (0.009-0.08) to (0.009-0.16) Hz (as observed in case of non- normalized data).
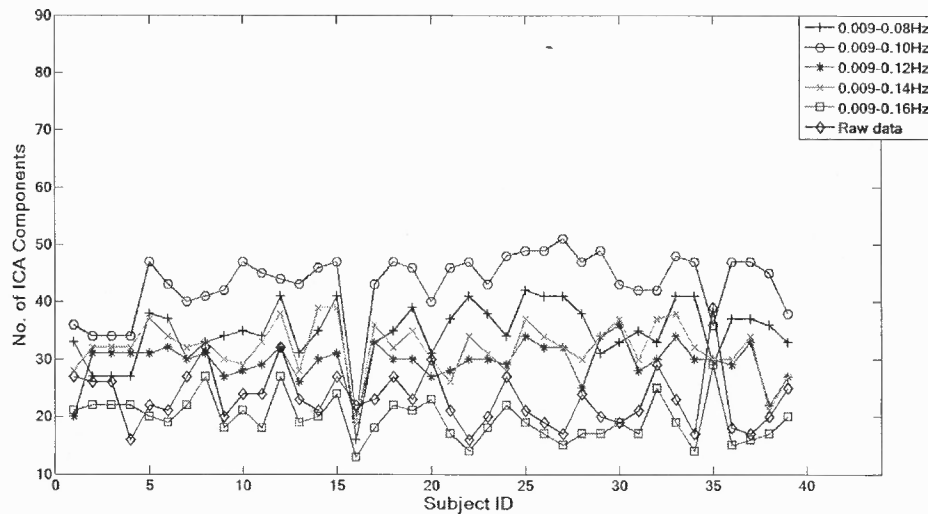

Figure 4.11 Number of independent components for each subject from temporal filtering using Rectangular filter. Each curve represents a different frequency range used for band pass filter design (ICA data-preprocessing was done after converting data into MNI space).

Following Figure 4.12 shows the plot of number of ICA components for spatial smoothing using different filters and figure 4.13 shows the plot for ICA components for spatial smoothing using Gaussian blur with different FWHM for the data set normalized to standard brain MNI space.
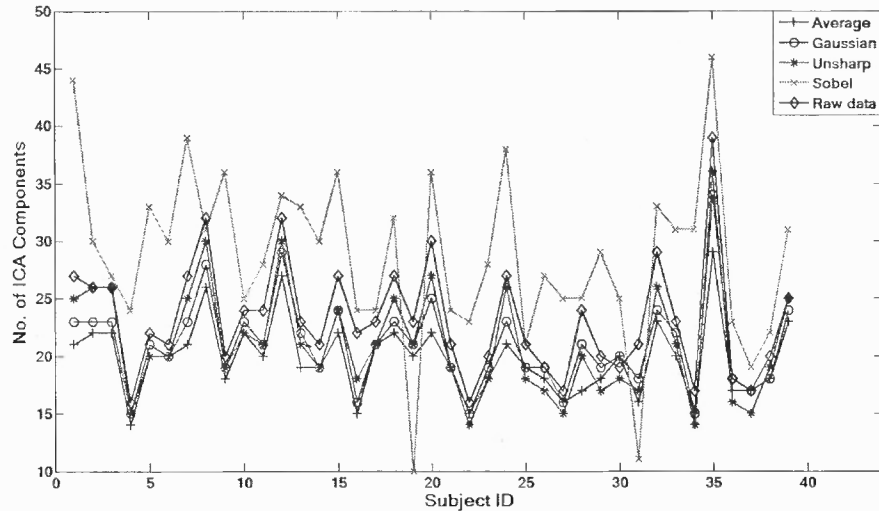
Figure 4.12 Plot of number of independent components for each subject for spatial smoothing using Average, Gaussian, Unsharp and Sobel filters after converting into MNI space.

4.2   Discussions

The results obtained for motion correction show no significant difference for different types of interpolations - Fourier, Quintic, Cubic, Heptic or Clipit. The number of ICA components was found to be same for various motion correction algorithms. However it was suggested by Cox et al that Fourier is the most accurate and Cubic was the fastest though least accurate but none of these algorithms methods showed any difference for our dataset. Also, we did not observe much motion in any of the subjects either. So it can be inferred that any of these methods maybe used for motion correction for resting state dataset in the study. A pattern was observed in case of temporal filtering of non-normalized data using either Hamming or Gaussian filter. The number of ICA components follows an increasing trend with increasing limit of low pass cut off frequency bandwidth. However, when compared with the raw data, number of components in raw data of each subject was much less in comparison to any of the

filtering band width (0.001-0.16) Hz. Then, the same analysis method was performed for single subjects increasing the bandwidth further than (0.009-0.16) Hz in small steps. It was observed that after a definite cutoff frequency at around 0.2Hz, number of components started decreasing sharply and then it came to saturation as shown in figures 4.13. A similar figure 4.14 confirms that this was indeed the case for other subjects as well. Recognizing that the frequency of respiration is around 0.20 Hz for normal human being, that causes an increase in the variability and thus the number of independent components decreases. The effect of increasing bandwidth tested on one subject is shown in following figure 4.13 and was then compared with another subject in figure 4.14. Filtered results were seen to be similar for both subjects considered for this comparison.
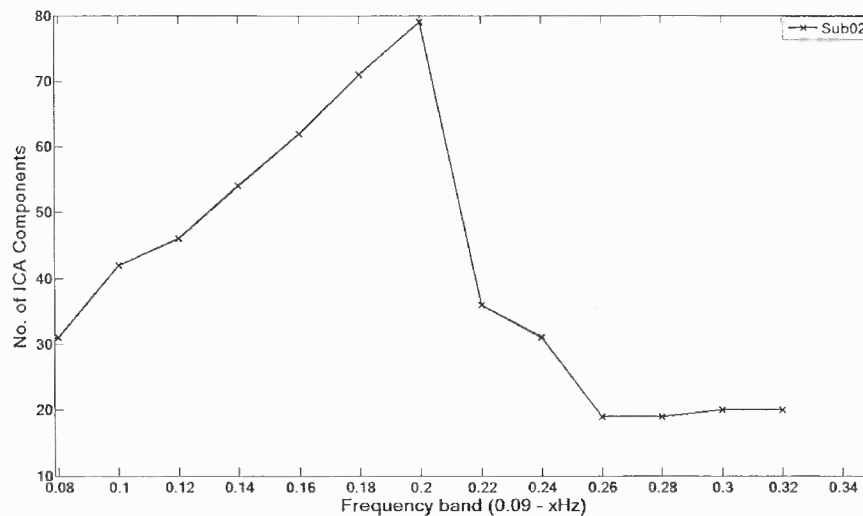

Figure 4.13 Number of independent components for subject # 02 from temporal filtering using Gaussian filter.
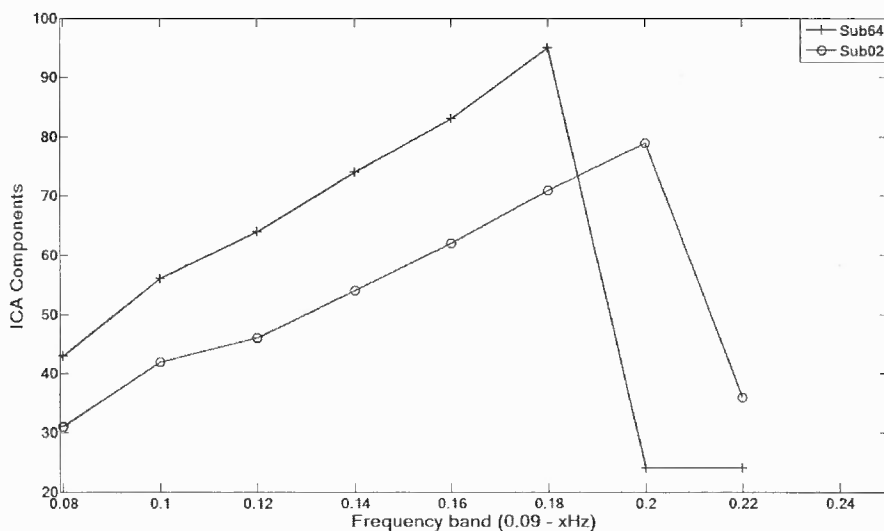
Figure 4.14 Number of independent components from temporal filtering using Gaussian filters shown for subject#02 and subject#34.

The respiration effect can also be seen at frequencies around .15 Hz in data converted into normalized MNI space which was earlier than for the case of non-normalized data. Therefore it is suggested, to be on a safer side, not to use a cutoff frequency above .12 Hz for resting state data.On comparing the response of different type of filters used for temporal filters, no systematic changes pattern was observed for Rectangular filter. This could be due to the large side lobes in frequency response of the Rectangular filter. It can also be inferred that Hamming filter was more sensitive to the respiratory effect as change in the pattern is visible at .14 Hz but for Gaussian it is more prominent at frequency of .16 Hz (refer figures 4.2 and 4.3). Figures 4.15 and 4.16 compare the response of all three Hamming, Gaussian and Rectangular filter for a fixed frequency bandwidth (0.009-0.08) Hz. Figure 4.17 show the time series obtained by each of these filters.
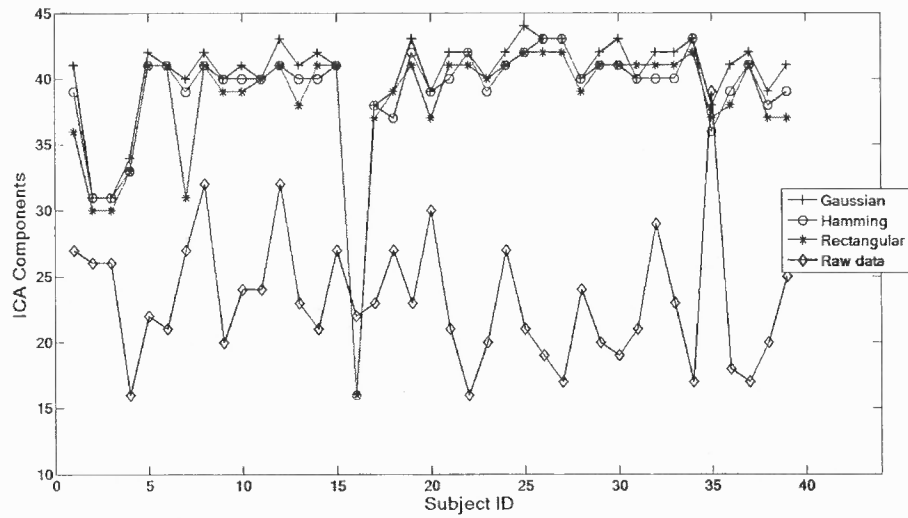
Figure 4.15 Comparison between Gaussian, Hamming and Rectangular filter at frequency bandwidth (0.009-0.08) Hz
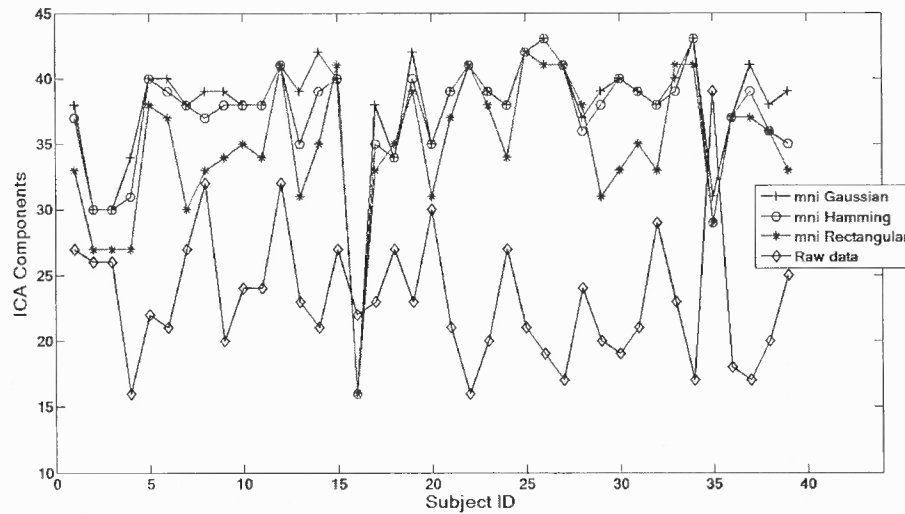

Figure 4.16 Comparison between Gaussian, Hamming and Rectangular filter at frequency bandwidth (0.009-0.08) Hz for data converted to MNI space
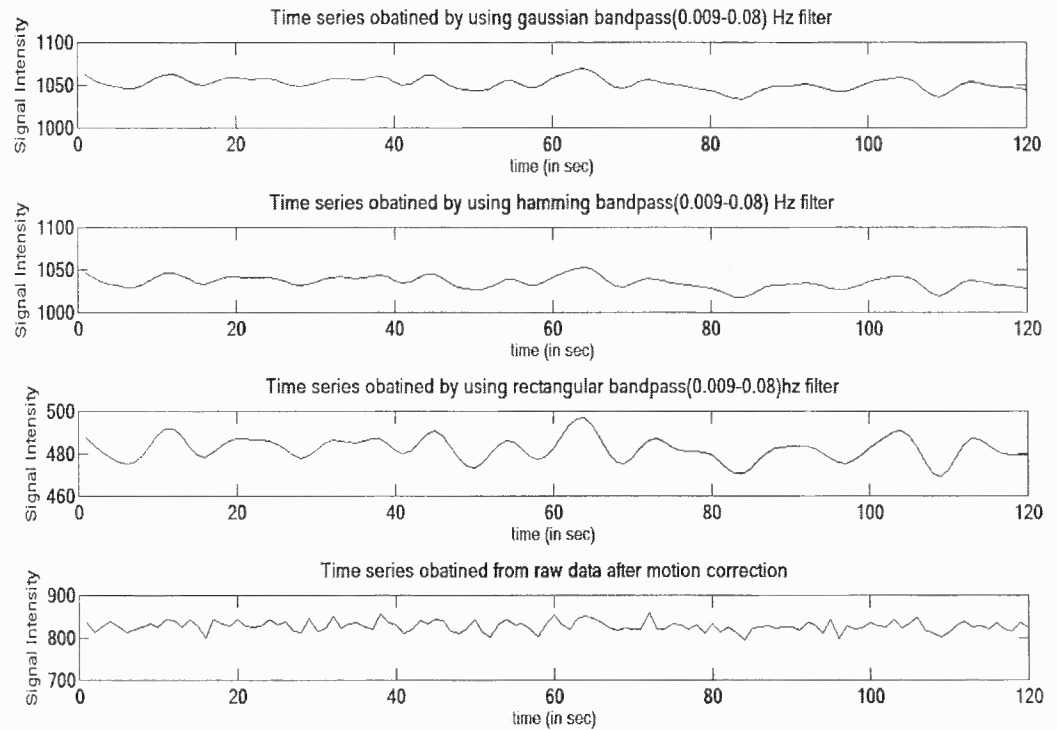
Figure 4.17 Time series obtained after different temporal filters

Also, spatial smoothing was performed using different types of filters along with changing their parameters. Figure 4.5 under results section, shows that the resultant number of ICA components doesn't reflect significant difference when Average or Gaussian filters are used. For Unsharp filtering however there is slight increase in number of components but for Sobel it increases drastically. This could be because both Sobel and Unsharp fileter are highpass filters, where Sobel filter emphasizes more on edge smoothing and is less sensitive to noise whereas Unsharp smoothing sharpens the edges. Figure 4.18 shows preprocessed data output for each of these smoothing methods.

Also the effect of smoothing can be compared for smoothing parameters as shown in the figure 4.19. It can be seen that with increasing matrix size, the resolution is affected
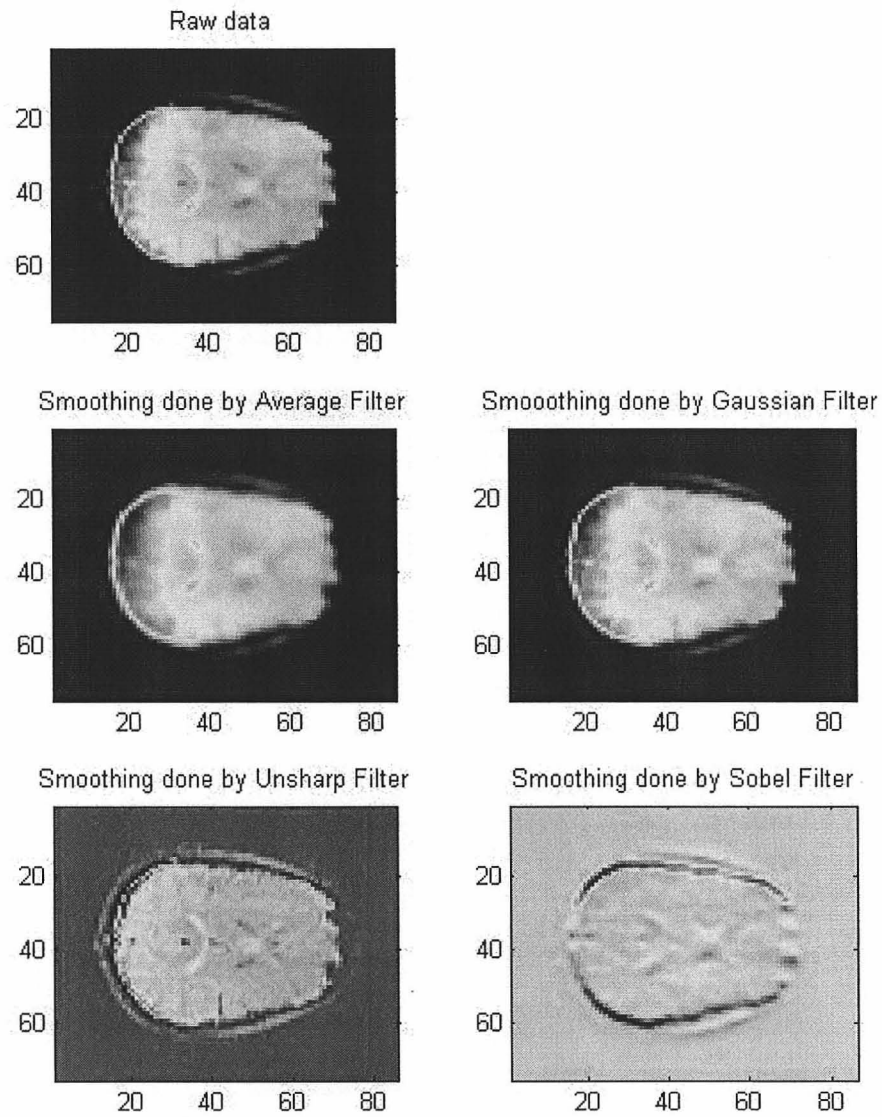
adversely.

Figure 4.18 Comparison of preprocessed images obtained from smoothing using different types of filters

So although there isn't significant difference between the number of components obtained by using matrix size [3 3] and [5 5] but for matrix size [7 7] it looked significantly different. Just by looking at images it can be believed that using a bigger size matrix like [7 7] (similar to using higher value for FWHM, say 8) is definitely not a good idea. Whereas it doesn't make much difference between using [3 3] or [5 5] however some information is certainly lost in [5 5]. Therefore, matrix size of [3 3] should be an optimal solution for smoothing.
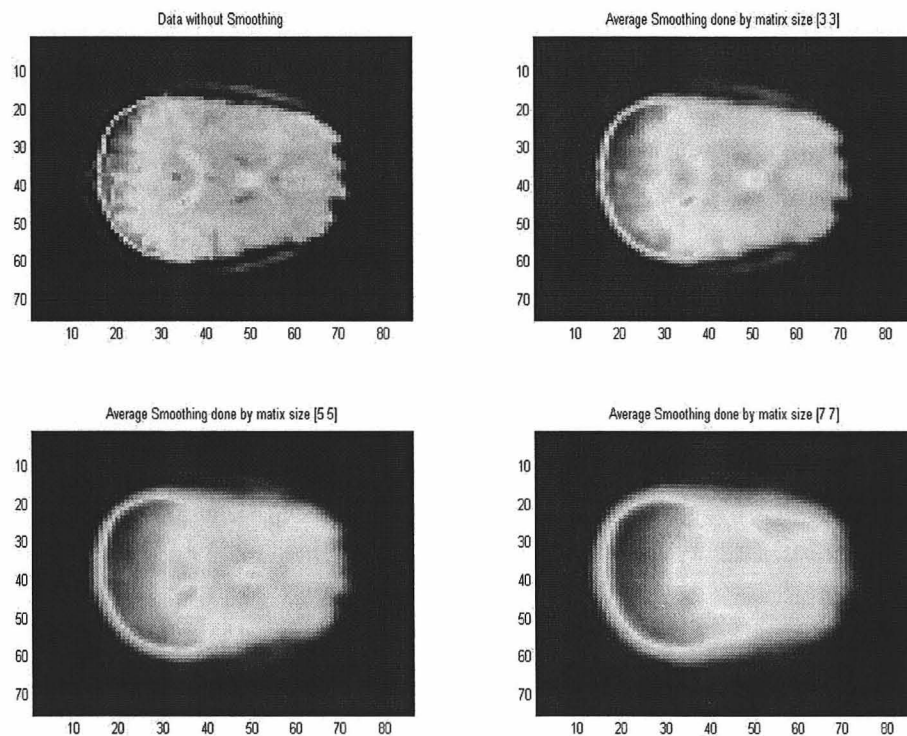

Figure 4.19 Images obtained from Average smoothing using different matrix size
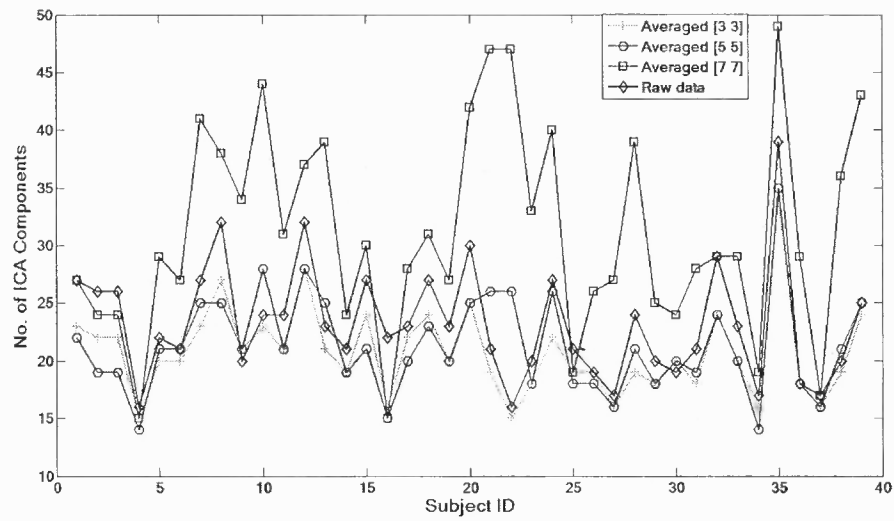
Figure 4.20 Number of components for Average type smoothing obtained by using different matrix size

From our discussion above it appears that using Sobel or Unsharp filters for spatial smoothing should not be advisable. At the same time, it can also be seen that both Average and Gaussian filters results in similar connectivity maps. However, by closely observing at their frequency response, both Average and Gaussian, one can see that both filters attenuate higher frequency contents of the signal more as compared to low frequency contents. But Average filter exhibits oscillations in its frequency response whereas Gaussian shows no side lobes. We should be careful to avoid such oscillating behavior and to ensure about the frequency range present in the images and attenuated from the images. Therefore, Gaussian filter should be preferred over Average filter for resting state data smoothing.

CHAPTER 5

CONCLUSIONS

ICA is reliable technique as long as we have sufficient data for probability based analysis. When the problems and conditions get specific to a small set of data, we cannot use ICA for making any intelligent decisions, but in all other cases ICA provides very good estimate of effects of each step of preprocessing.

While preprocessing the resting state fMRI data, it is found that motion correction is insignificant in this case and it doesn't matter which motion correction technique is used. For spatial smoothing of the resting state fMRI data, a low pass filter would be required. For temporal filtering, a band-pass filter with higher cut-off frequency less than 0.12Hz is desirable. Gaussian or Hamming filters, both work effectively for temporal filtering. However a high order filter should be avoided.

REFERENCES

[1]   Belliveau JW, Kennedy DN, McKinstry RC, et al. (1991) Functional mapping of the human visual cortex by magnetic resonance imaging. Science, 1:254(5032):716 -719.

[2]   Ogawa S, Tank DW, Menon R, Ellermann JM, Kim SG, Merkle H, Ugurbil K (1992) Intrinsic signal changes accompanying sensory stimulation: functional brain mapping with magnetic resonance imaging. Proc Natl Acad Sci USA, 1:89(13):5951-5955.

[3]   Biswal BB, Yetkin FZ, Haughton VM, Hyde JS (1995) Functional connectivity in the motor cortex of resting human brain using echo-planer MRI. Magnetic Resonance in Medicine, 34(4): 537-541.

[4]   Buckner RL, Andrews-Hanna JR, Schacter D (2008) The Brain's Default Network Anatomy, Function and Relevance to disease. Annals of the New York Academy of Sciences, 1124: 1-38.

[5]   Broyd SJ, Demanuele C, Debener S, Helps SK, James CJ, Sonuga-Barke EJS (2009) Default-mode brain dysfunction in mental disorders: A systematic review. Neuroscience and Biobehavioral Reviews, 33(3): 279-296.

[6]   Worsley KJ, Friston KJ (1995) Analysis of fMRI time-series revisited - Again NeuroImage, 2(3): 173-181.

[7]   Triantafyllou C, Hoge RD and Wald LL (2006). Effect of spatial smoothing on physiological noise in high-resolution fMRI. NeuroImage, 32(2):551-557.

[8]   Bianciardi M, Cerasa A, Patria F, Hagberg GE (2004). Evaluation of mixed effects in event-related fMRI studies: Impact of first-level design and filtering. NeuroImage, 22(3):1351-1370.

[9]   Kruggel F, Von Cramon DY, Descombes X (1999). Comparison of filtering methods for fMRI datasets. NeuroImage, 10(5):530-543.

[10]   De Luca M, Beckmann CF, De Stefano N, Matthews PM, Smith SM (2006). fMRI resting state networks define distinct modes of long-distance interactions in the human brain. NeuroImage, 29(4):1359-1367.

[11]   Beckmann CF and Smith SM (2004) Probabilistic Independent Component Analysis for Functional Magnetic Resonance Imaging.IEEE Trans. on Medical Imaging, 23(2):137-152.

[12] Oakes T.R., Johnstone T., Ores Walsh K.S., Greischar L.L., Alexander A.L., Fox A.S., Davidson R.J. (2005). Comparison of fMRI motion correction software tools. NeuroImage, 28(3):529-543.

[13] Eddy WF, Fitzgerald M, Noll DC (1996). Improved Image Registration by Using Fourier Interpolation. Magnetic Resonance in Medicine, 36(6): 923-931.